The Mechanism of Alkene Addition to a Nickel Bis(dithiolene) Complex: The Role of the Reduced Metal Complex

Li Dang,[†] Mohamed F. Shibl,[‡,||] Xinzheng Yang,[†,⊥] Aiman Alak,[§] Daniel J. Harrison,[§] Ulrich Fekl,*[,§] Edward N. Brothers,*[,‡] and Michael B. Hall*[,†]

[†]Department of Chemistry, Texas A&M University, College Station, Texas 77842, United States
[‡]Department of Chemistry, Texas A&M University at Qatar, Doha, Qatar
[§]University of Toronto Mississauga, Mississauga, Ontario, Canada L5L 1C6
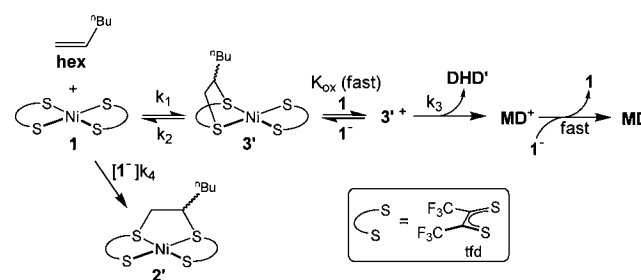
S *Supporting Information*

ABSTRACT: The binding of an alkene by Ni(tfd)$_2$ [tfd = S$_2$C$_2$(CF$_3$)$_2$] is one of the most intriguing ligand-based reactions. In the presence of the anionic, reduced metal complex, the primary product is an interligand adduct, while in the absence of the anion, dihydrodithiins and metal complex decomposition products are preferred. New kinetic (global analysis) and computational (DFT) data explain the crucial role of the anion in suppressing decomposition and catalyzing the formation of the interligand product through a dimetallic complex that appears to catalyze alkene addition across the Ni–S bond, leading to a lower barrier for the interligand adduct.

Nonconventional (ligand-based) reactions of sulfur-containing metal complexes with alkenes have attracted significant attention[1−5] ever since the early studies on the reactions of metal bis(dithiolene) complexes with strained and cyclic alkenes in the 1960s.[6] A 2001 paper on binding of simple alkenes such as ethylene to Ni(tfd)$_2$ (**1**) [tfd = S$_2$C$_2$(CF$_3$)$_2$], for potential use as a separation method for petroleum feedstocks, created substantial excitement.[1] However, a key step in the separation, namely, the formation of stable adducts, is difficult; a recent study showed that metal complex decomposition (to give **MD**) occurs for both ethylene and 1-hexene (via **3** and **3′**, respectively; Scheme 1).[4] The same study showed that the presence of the reduced metal complex **1**$^−$ changes the product selectivity in favor of the stable adducts **2** and **2′**, respectively (Scheme 1). The mechanism, in particular regarding the role of the anion, remained speculative. A previous theoretical study on neutral systems predicted that the formation of the cis interligand adduct could potentially circumvent the symmetry constraints via a two-step process in which a twisted (pseudotetrahedral) adduct forms and then isomerizes to the more thermodynamically stable square-planar product.[7] However, the role of the anion was not known or considered at that time and has not yet received either quantum-chemical study or detailed kinetic analysis. In this work, the reaction mechanism was investigated using a combination of kinetics *and* computations.

To study the binding of 1-hexene (**hex**) to **1** in CDCl$_3$ at room temperature, 24 time traces[8] were obtained and simultaneously fit to various models (global analysis) using the DynaFit program.[9] The model that fit best was catalysis of **2′** formation by **1**$^−$ in a "parallel reactions" model [Scheme 2;
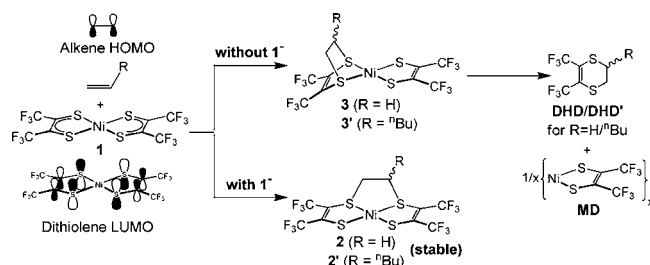
Scheme 2

the other models are described in the Supporting Information (SI)]. In this model, if enough **1**$^−$ is available, formation of **2′** can become competitive with formation of **3′**. The best-fit parameters for this model (k_1–k_4 and K_{ox}) were globally optimized using all of the available data points. Figure 1 shows the experimental data points and the fit, with the numerical results given in the legend. The average absolute deviation between the fitted curves and raw data was on the order of 10%, which is reasonable for concentrations that were obtained from manual integration of NMR intensities.[10]

Another mechanism that was investigated was an "isomerization model" in which **3′** (cf. Scheme 1) is a common intermediate that would decompose in the absence of **1**$^−$ or isomerize to form **2′** in the presence of **1**$^−$. Both basic three-
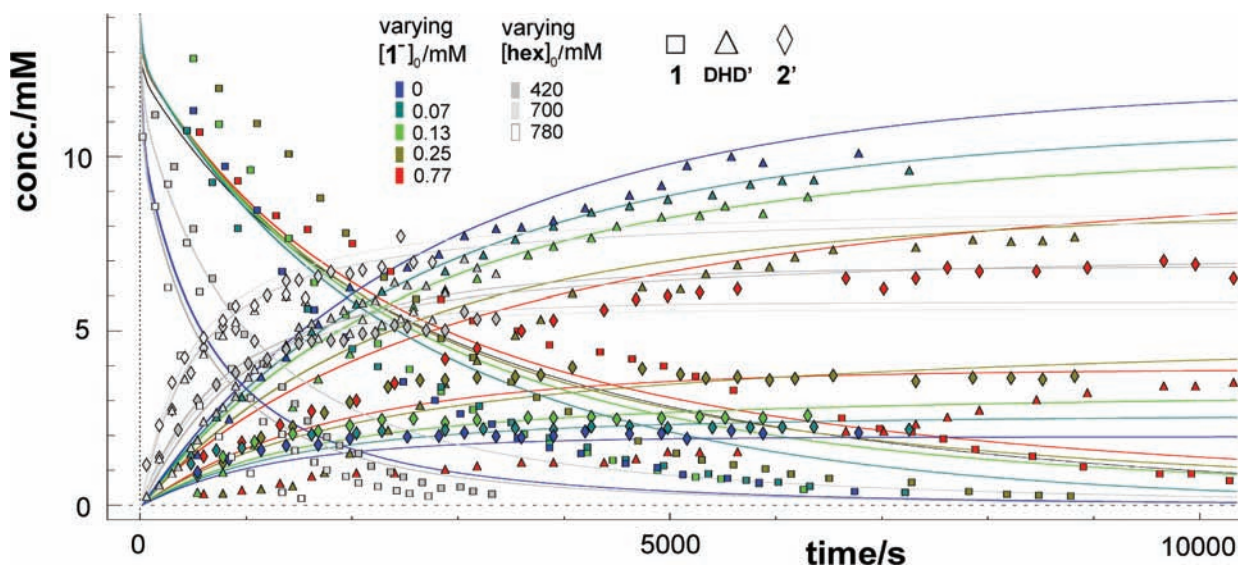
Scheme 1

Figure 1. Global simultaneous fit (curves shown) of the model shown in Scheme 2 to the set of 24 time traces for **1** (squares), **DHD′** (triangles), and **2′** (diamonds) obtained using varying initial concentrations $[\mathbf{1}^-]_0$ and $[\mathbf{hex}]_0$ (**hex** = 1-hexene) at 298 K in CDCl$_3$. $[\mathbf{1}]_0$ was always between 13.2 and 14.0 mM (exact values are given in the SI). When $[\mathbf{1}^-]_0$ was varied (data points in color), $[\mathbf{hex}]_0$ was 140 mM. For $[\mathbf{1}^-]_0 = 0$, a value of 1×10^{-6} mM was used as input (instead of exactly zero) to avoid a "division by zero" error. When $[\mathbf{hex}]_0$ was varied (data points in shades of gray), $[\mathbf{1}^-]_0$ was 0.25 mM. Fitted values of the parameters: k_1, $1.3(7) \times 10^{-5}$ mM^{-1} s^{-1}; k_2, $5(4) \times 10^{-2}$ s^{-1}; K_{ox}, $5(2) \times 10^{-2}$; k_3, $9.5(8) \times 10^{-3}$ s^{-1}; k_4, $1.91(8) \times 10^{-6}$ mM^{-2} s^{-1}.

parameter and more sophisticated five-parameter isomerization models provided fits that were far inferior to that for the "parallel reactions" model (the reaction schemes and data fitting are shown in the SI). The "parallel reactions" model (Scheme 2, Figure 1) is thus strongly favored. Aspects of this model are easily judged to be realistic. It requires the intraligand addition step to be reversible (second-order k_1, first-order k_2), which has been observed for a related molybdenum tris(dithiolene) complex.[3] More distantly related adducts to P,S-ligands show extremely rapid reversibility.[2] In addition, oxidation of the intraligand adduct **3′** to form a cationic species (K_{ox}) is reasonable, as **3′** contains a true ene-1,2-dithiolate, which should make it easy to oxidize. While no sulfur-based species that is very similar to **3′** can be obtained as a stable species, related nitrogen-chelated compounds (N^N)-Ni(S$_2$C$_2$(CF$_3$)$_2$) are known and undergo oxidation at potentials close to the redox potential for **1**/**1**$^-$.[11] In regard to the final electron-transfer step, polymeric/oligomeric metal decomposition products were observed by NMR spectroscopy, and in the model the simplifying assumption was made that **MD**$^+$ is rapidly and completely reduced by **1**$^-$ to regenerate **1**. We note that incomplete reduction under some conditions would be an excellent explanation for Geiger's observation[12] that small amounts of **1**$^-$ are produced in the reaction of neutral **1** with norbornadiene.

For the formation of the stable adduct **2′**, we modeled a "step" that is overall third-order: first-order in **1**, first-order in **hex**, and first-order in **1**$^-$ (Scheme 2; this step is catalytic in **1**$^-$, since **1**$^-$ is regenerated in this step).[13] This is not meant to imply a trimolecular encounter. An overall third-order dependence would be observed if two of the species form an association complex, which then reacts with the third species. It was previously suggested[4] that **1**$^-$ might bind **hex** to form **2′**$^-$ and then be subsequently reoxidized by **1**. However, computations indicate that the formation of **2**$^-$ is energetically unfavorable (see the SI).

Our new density functional theory (DFT) data now provide a convincing explanation that is detailed below: **1**$^-$ binds **1** to form a dimetallic complex, which then reacts with the alkene. While analysis of the kinetic data showed that **1**$^-$ catalyzes the formation of the stable interligand adduct in a step that depends on $k_4[\mathbf{1}][\mathbf{1}^-][\mathbf{hex}]$, the exact mechanism was clarified by the theoretical work. DFT calculations on the reactions in Schemes 1 and 2[14−22] were performed for ethylene, and the results are presented in Figures 2 and 3. In the absence of anion (Figure 2), the cis interligand adduct **2** can be formed via direct addition of **1** with ethylene by overcoming a barrier of 26.0 kcal/mol to form the twisted cis interligand intermediate (**2y**), which is the previously modeled symmetry-allowed interligand
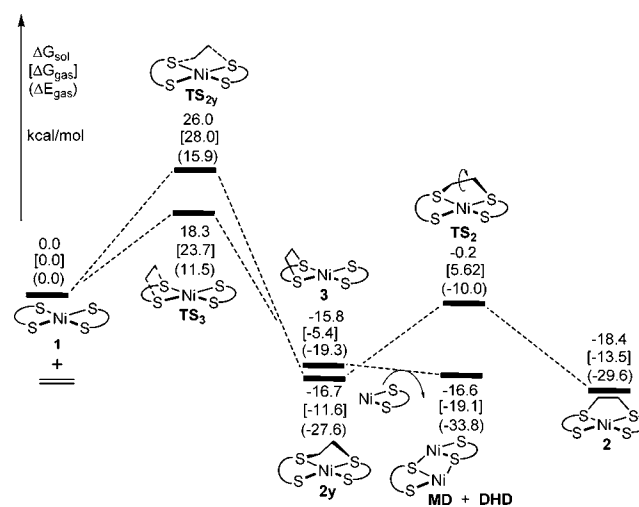

Figure 2. Energy profile for the reactions of **1** with ethylene to form interligand adducts **2y** and **2**, the intraligand adduct **3**, and the decomposition products **DHD/MD**. Relative free energies in solvent, free energies in the gas phase [in square brackets], and electronic energies in the gas phase (in parentheses) in kcal/mol are shown.

Figure 3. Free energy profile for the formation of **2** and **1⁻** via **D0⁻**, **D1⁻**, **D2⁻**, and **4**. For **TS_{D12}⁻**, a scan of the relaxed PES from **D2⁻** along the Ni−C, S−C distance showed that the PES is flat from **D2⁻** to **TS_{D12}⁻**. Relative free energies in solvent, free energies in the gas phase [in square brackets], and electronic energies in the gas phase (in parentheses) in kcal/mol are shown.
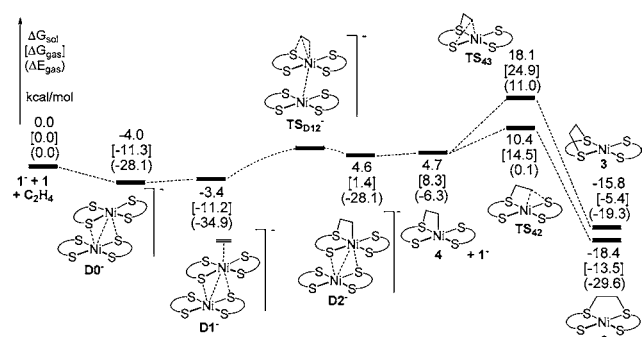
route.[7] **2y** then isomerizes to give the thermodynamically more stable **2** with a barrier of 16.5 kcal/mol. However, as expected from the experiments detailed above, the barrier for formation of the intraligand adduct (**3**) was calculated to be lower than the maximum barrier leading to **2**; the DFT work gave a difference of 7.7 kcal/mol. The intraligand adduct **3** subsequently decomposes to **DHD** (observed) and **MD** (a mix of oligomers observed). For computational simplicity, **MD** was modeled as a dimer only. The lower barrier for formation of **3** is the reason for decomposition when no anion is present.

However, when **1⁻** is present, the formation of a dimetallic complex (**D0⁻** in Figure 3) from **1** and **1⁻** is favorable, and **D0⁻** reacts with ethylene to give **D1⁻**; ethylene then migrates to form **D2⁻**. When **D2⁻** dissociates, **1⁻** is regenerated, and a compound with ethylene bonded to the nickel and one sulfur (**4**) results. **4** is more readily transformed into **2** than into **3**, via a barrier of 5.7 kcal/mol (vs 13.4 kcal/mol). The formation of **4** from **1**, **1⁻**, and ethylene via dimetallic complexes thus provides a route for **1⁻** to act as a catalyst for the production of **2**.[23] Although the binding of the alkene to **D0⁻** to form the initial alkene adduct (**D1⁻**) is weak, the transition between the initial adduct and the species with the alkene added across the Ni−S bond (**D2⁻**) occurs on an extremely flat potential energy surface (PES): a small movement of the alkene in **D2⁻** resulted in optimization to **D1⁻**. Because the isomerization of species **4** has a smaller barrier for production of **2** (compared with the barrier for production of **3**), an overall changeover in selectivity results in the presence of the reduced metal complex. The novel catalytic cycle involving dimetallic complexes thus puts new emphasis on weakly associated dinuclear complexes in the reactivity of nickel bis(dithiolene) complexes.
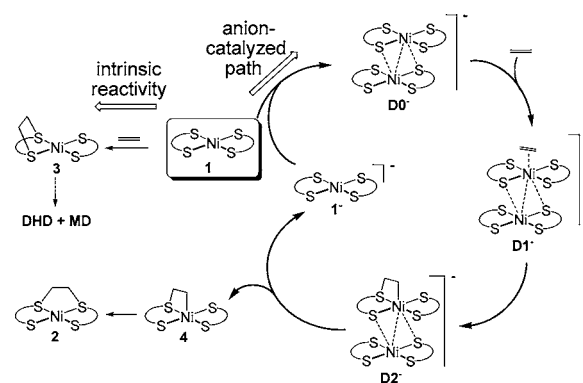
While dimerization is common for bis(dithiolene) complexes of cobalt and iron,[24] association in solution is rare for nickel triad bis(dithiolene) complexes. However, oligomerization was proposed as the reason for the electrochemical irreversibility in the oxidation of Pd(mnt)₂⁻ [mnt = S₂C₂(CN)₂] and also as the underlying reason for the difficulty in obtaining pure Ni(mnt)₂ via electrochemical oxidation of the anion in concentrated solution.[25] To supplement the computational evidence for the dimetallic species **D0⁻** with direct experimental evidence,[26] we performed electrospray ionization mass spectrometry (ESI-MS; negative ion mode in acetonitrile) on an equimolar mixture of **1** and (**1⁻**)(NEt₄⁺). A signal with the expected isotope signature

indicative of the acetonitrile adduct of **D0⁻** ($C_{18}H_3F_{24}N_1Ni_2S_8^-$) was obtained (see the SI).

The computational results are also consistent with the proposal that decomposition (via **3**/**3⁺**) is slowed in the presence of **1⁻**. The reduction potential for **1**/**1⁻** is less positive but relatively close to the computed reduction potential for **3⁺**/**3** (electron transfer from **3** to **1** is uphill by 10.7 kcal/mol = 464 mV; the calculated thermodynamic data and reduction potentials vs ferrocenium/ferrocene are given in the SI),[27] indicating that **3⁺** formation can be suppressed in the presence of **1⁻**. Species **3⁺** exhibits longer Ni−S bonds to **DHD** than does **3**, which might indicate that **DHD** becomes more labile after oxidation of **3**, although the effect is very small (0.0015 Å). In addition, since substitution is often associative for Ni(II),[28] it can be expected that **DHD** loss (decomposition) is faster for cationic **3⁺**.

In conclusion, this combination of experiment and theory has elucidated the mechanism for the ligand-based reaction between alkenes and Ni(tfd)₂ (**1**), where catalytic amounts of **1⁻** lead to a change in selectivity. The intrinsic reactivity of **1** favors the unstable intraligand adduct, which is formed in a symmetry-allowed reaction. Kinetic data have provided evidence for the **1⁻**-catalyzed formation of the stable interligand adduct, and DFT studies have shown the reason: **1⁻** combines with **1** to form a dimetallic intermediate, which then binds ethylene at one of the nickel atoms. A low-energy isomerization yields a complex in which ethylene is bound across the Ni−S bond and **1⁻** is released. The short-lived Ni−S alkene adduct isomerizes more rapidly to the (stable) interligand adduct than to the (unstable) intraligand adduct. The anion-catalyzed reaction thus competes effectively with the intrinsic reactivity of **1**, as shown in Scheme 3. In view of the recent interest in ligand-based alkene reactions, this analysis of prototypical Ni(tfd)₂ reactivity will aid in future work in this area.

Scheme 3

■ ASSOCIATED CONTENT

Ⓢ Supporting Information

Complete ref 18; gas-phase electronic energies and atomic coordinates of optimized intermediates and transition states; Dynafit script and raw kinetic data, along with analysis of the fitting results; and ESI-MS data. This material is available free of charge via the Internet at http://pubs.acs.org.

AUTHOR INFORMATION

Corresponding Author

ulrich.fekl@utoronto.ca;   edward.brothers@qatar.tamu.edu;
hall@chem.tamu.edu

Present Addresses

$^{\parallel}$On sabbatical from the Faculty of Science, Department of Chemistry, Cairo University, Giza, Egypt.
$^{\perp}$Molecular Graphics and Computation Facility, College of Chemistry, University of California, Berkeley, CA 94720.

Notes

The authors declare no competing financial interest.

REFERENCES

(1) Wang, K.; Stiefel, E. I. *Science* **2001**, *291*, 106.
(2) (a) Grapperhaus, C. A.; Ouch, K.; Mashuta, M. S. *J. Am. Chem. Soc.* **2009**, *131*, 64. (b) Ouch, K.; Mashuta, M. S.; Grapperhaus, C. A. *Inorg. Chem.* **2011**, *50*, 9904.
(3) Harrison, D. J.; Lough, A. J.; Nguyen, N.; Fekl, U. *Angew. Chem., Int. Ed.* **2007**, *46*, 7644.
(4) Harrison, D. J.; Nguyen, N.; Lough, A. J.; Fekl, U. *J. Am. Chem. Soc.* **2006**, *128*, 11026.
(5) Nguyen, N.; Harrison, D. J.; Lough, A. J.; De Crisci, A. G.; Fekl, U. *Eur. J. Inorg. Chem.* **2010**, 3577.
(6) (a) Schrauzer, G. N.; Mayweg, V. P. *J. Am. Chem. Soc.* **1965**, *87*, 1483. (b) Wing, R. M.; Tustin, G. W.; Okamura, W. H. *J. Am. Chem. Soc.* **1970**, *92*, 1935.
(7) Fan, Y.; Hall, M. B. *J. Am. Chem. Soc.* **2002**, *124*, 12076.
(8) The 24 time traces were from eight different kinetic runs (459 total data points) in which the **1**$^-$ and **hex** concentrations were varied. In each run, the concentrations of the three directly observable (long-lived and NMR-active) species **1**, **DHD′**, and **2′** were monitored by ^{19}F NMR spectroscopy.
(9) DynaFit, version 3.28: Kuzmič, P. *Anal. Biochem.* **1996**, *237*, 260.
(10) However, there was a small systematic deviation at early reaction times, particularly for runs involving high concentrations of **1**$^-$: an initially low rate (induction period) was observed for formation of **DHD′** that was underestimated by the model. While the model chosen allows for an induction period for **DHD′** production (because **DHD′** is "stored" in the form of **3′/3′$^+$** before **DHD′** can be produced), the final curve fit somewhat underestimated the magnitude of the effect. It is conceivable that the more pronounced induction period in the experimental data relative to the model could be an experimental artifact arising from underestimation of small concentrations of **DHD′** due to line broadening in the sample, which became more paramagnetic at higher **1**$^-$ concentrations. A tighter fit to the curves showing the sigmoidal (induction period) behavior was obtained when those curves were fit individually, but the overall best parameters are, of course, not those obtained from local optimization of selected curves but those from global optimization using all of the curves, which was the method chosen and shown in Figure 1.
(11) Miller, T. R.; Dance, I. G. *J. Am. Chem. Soc.* **1973**, *95*, 6970.
(12) Geiger, W. E. *Inorg. Chem.* **2002**, *41*, 136.
(13) Making this step only second-order degraded the quality of the fit.
(14) All calculations were done with ωB97XD,[15] which produced[16] relative energies similar to CCSD[17] for the reaction of ethylene with Ni(S$_2$C$_2$H$_2$)$_2$. Gaussian 09[18] was used, and an all-electron 6-31++G** Pople basis set[19] was specified for H, C, F, S, and Ni atoms; this specification uses the Wachters−Hay basis set for Ni.[20] All of the geometries used were optimized in the gas phase, and vibrational frequencies confirmed the nature of all intermediates and transition states. The latter were confirmed by intrinsic reaction coordinate (IRC) calculations.[21] The solvation effects in chloroform were simulated using the SMD solvent model.[22] We calculated the solution-phase free energy (ΔG_{sol}) by adding solvation energies to the gas-phase relative free energies (ΔG_{gas}). Unless specified, the ΔG_{sol} values have been used in the discussion. Ethylene was used in place of 1-hexene for computational efficiency.
(15) Chai, J. D.; Head-Gordon, M. *Phys. Chem. Chem. Phys.* **2008**, *10*, 6615.
(16) Dang, L.; Yang, X.; Brothers, E. N.; Hall, M. B. *J. Phys. Chem. A* **2011**, *116*, 476.
(17) (a) Cizek, J. *Adv. Chem. Phys.* **1969**, *14*, 35. (b) Purvis, G. D., III; Bartlett, R. J. *J. Chem. Phys.* **1982**, *76*, 1910. (c) Scuseria, G. E.; Janssen, C. L.; Schaefer, H. F., III. *J. Chem. Phys.* **1988**, *89*, 7382. (d) Scuseria, G. E.; Schaefer, H. F., III. *J. Chem. Phys.* **1989**, *90*, 3700.
(18) Frisch, M. J.; et al. *Gaussian 09*; Gaussian, Inc.: Wallingford, CT, 2009.
(19) Krishnan, R.; Binkley, J. S.; Seeger, R.; Pople, J. A. *J. Chem. Phys.* **1980**, *72*, 650.
(20) (a) Wachters, A. J. H. *J. Chem. Phys.* **1970**, *52*, 1033. (b) Hay, P. J. *J. Chem. Phys.* **1977**, *66*, 4377.
(21) (a) Fukui, K. *J. Phys. Chem.* **1970**, *74*, 4161. (b) Fukui, K. *Acc. Chem. Res.* **1981**, *14*, 363.
(22) Marenich, A. V.; Cramer, C. J.; Truhlar, D. G. *J. Phys. Chem. B* **2009**, *113*, 6378.
(23) Many alternative pathways that were found to be unfavorable because of unstable products or high barriers (such as the formation of **4** in the absence of **1**$^-$) will be discussed in a full article in the near future.
(24) (a) Balch, A. L.; Dance, I. G.; Holm, R. H. *J. Am. Chem. Soc.* **1968**, *90*, 1139. (b) Jacobsen, H.; Donahue, J. P. *Inorg. Chem.* **2008**, *47*, 10037.
(25) Geiger, W. E.; Barrière, F.; Lesuer, R. J.; Trupia, S. *Inorg. Chem.* **2001**, *40*, 2472.
(26) We thank one of the reviewers for this suggestion.
(27) See the SI. Ion pairing could potentially further stabilize the products. Also, it can be expected that the alkyl-substituted species **3′** is more easily oxidized than unsubstituted **3**.
(28) Cusumano, M.; Ricevuto, V. *J. Chem. Soc., Dalton Trans.* **1978**, 1682.